Title

Escherichia coli Attenuation by Fe Electrocoagulation in Synthetic Bengal Groundwater: Effect of pH and Natural Organic Matter

Journal

Environmental Science and Technology, 49(16)

ISSN

0013-936X

Authors

Delaire, Caroline
van Genuchten, Case M
Nelson, Kara L
et al.

Publication Date

2015-08-18

DOI

10.1021/acs.est.5b01696

Peer reviewed

Published in Environmental Sci. and Technology (ACS), July 2015.
DOI:10.1021/acs.est.5b01696

E. coli Attenuation by Fe Electrocoagulation in Synthetic Bengal Groundwater: Effect of pH and Natural Organic Matter

Caroline Delaire[a,*], Case M. van Genuchten[a,†], Kara L. Nelson[a], Susan E. Amrose[a], Ashok J. Gadgil[a,b]

[a] Department of Civil and Environmental Engineering, University of California, Berkeley, California, USA, 94720-1710

[b] Energy Technologies Area, Lawrence Berkeley National Laboratory, Berkeley, CA 94720, United States

[†]Current affiliation: Institut de Dynamiques de la Surface Terrestre, University of Lausanne, Lausanne, Switzerland

[*]Corresponding author: caroline.delaire@orange.fr

Abstract

Drinking water treatment technologies addressing both arsenic and microbial contamination of Bengal groundwater are needed. Fe electrocoagulation (Fe-EC), a simple process relying on the dissolution of an Fe(0) anode to produce Fe(III) precipitates, has been shown to efficiently remove arsenic from contaminated groundwater. We investigated *E. coli* attenuation by Fe-EC in synthetic Bengal groundwater as a function of Fe dosage rate, total Fe dosed, pH, and presence of natural organic matter (NOM). We demonstrated concurrent *E. coli* and arsenic attenuation, with a 2.5 mM Fe dosage achieving over 4-log *E. coli* attenuation and arsenic removal from 450 to below 10 μg/L. *E. coli* reduction was significantly enhanced at pH 6.6 compared to pH 7.5 (4.0 and 1.9 log respectively for a 0.5 mM Fe dosage), which we linked to the decreased rate of Fe(II) oxidation at lower pH. The presence of 3 mg/L-C of NOM (Suwanee River Fulvic Acid) did not significantly interfere with *E. coli* attenuation by Fe-EC. Based on live-dead staining, as well as on comparisons of *E. coli* reduction by Fe-EC and by coagulation with a ferric salt, we propose that the primary mechanism of *E.*

Published in Environmental Sci. and Technology (ACS), July 2015.
DOI:10.1021/acs.est.5b01696

coli attenuation by Fe-EC is physical removal with Fe(III) precipitate flocs, with inactivation likely contributing as well at lower pH. Transmission electron microscopy images showed that EC precipitates adhere to and bridge individual *E. coli* cells, resulting in large bacteria-Fe aggregates that can be removed by gravitational settling. Our results point to the unique ability of Fe-EC to treat a diverse range of chemical and biological contaminants simultaneously and suggest that groundwater remediation with Fe-EC in arsenic-affected areas may not need to be followed by a disinfection step.

Abstract Art

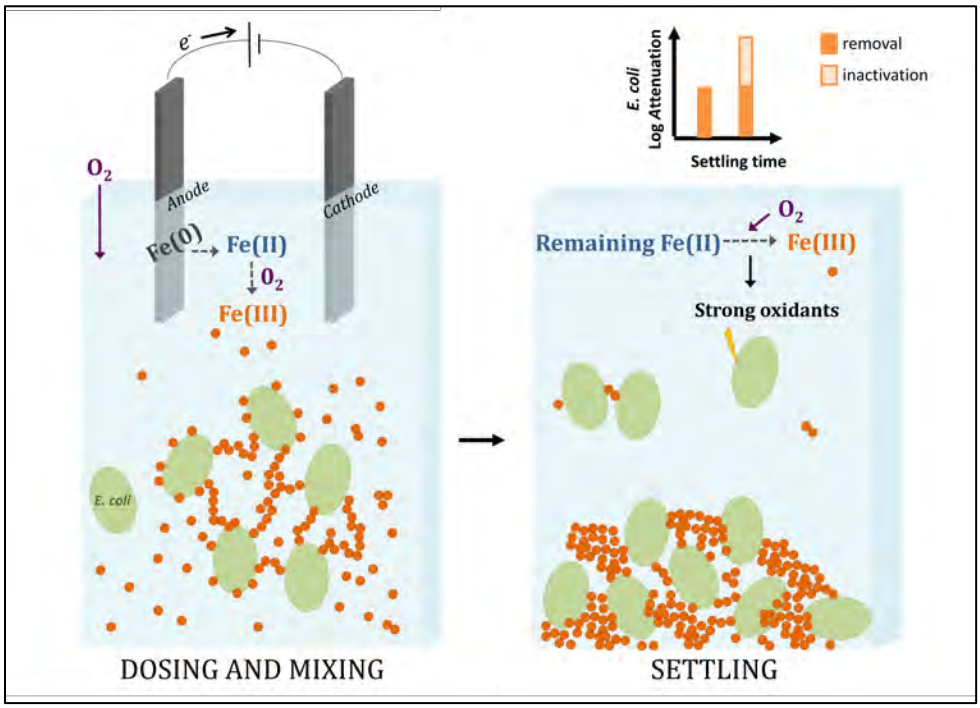

1. Introduction

Arsenic-contaminated groundwater serves as the primary drinking water source for tens of millions of people in Bangladesh and India[1]. Previous research aiming to improve the quality of arsenic-contaminated groundwater in the Bengal Basin has

focused on arsenic removal alone, largely ignoring possible concurrent microbial contamination of shallow aquifers. However, recent studies have reported the presence of fecal indicators and pathogens (rotavirus, *Shigella*, *Vibrio cholera*, pathogenic *E. coli* and adenovirus) in shallow tubewell water in Bangladesh[2–4]. A study of 125 tubewells in rural Bangladesh found that 30% of wells with arsenic levels above 50 μg/L had detectable levels of *E. coli*[2], indicating significant concurrent arsenic and fecal contamination. Although fecal contamination of groundwater is typically lower than that of surface water (fecal coliform concentrations in tubewells < 10^1-10^2 CFU/100 mL[2–7] compared to 10^2-10^4 CFU/100 mL in ponds and dug wells[5,8] and up to 200,000 CFU/100 mL in Ganga river[9]), it is suspected to contribute to the sustained prevalence of diarrheal diseases in the region[10,11]. These studies demonstrate the need for safe water solutions capable of addressing arsenic and microbial contamination simultaneously.

Iron electrocoagulation (Fe-EC) is a simple process that has been used to effectively remove arsenic from South Asian groundwater[12,13]. Fe-EC relies on the rapid dissolution of a sacrificial Fe(0) anode to produce Fe(II), which then oxidizes in the presence of dissolved oxygen to form Fe(III) precipitates with high specific surface area and a high affinity for arsenic adsorption[14]. Arsenic-laden precipitates can be removed subsequently by gravitational settling. In the EC process, strong oxidants generated in Fenton-type reactions convert As(III) into As(V), which is easier to remove at circumneutral pH[15]. Fe-EC effectively removes arsenic at low cost and is a realistic option for sustainable groundwater remediation in Bengal[16]. However, this technique has not been examined as a strategy for reducing the bacterial load in arsenic-contaminated

Published in Environmental Sci. and Technology (ACS), July 2015.
DOI:10.1021/acs.est.5b01696

water. Such examination is necessary to understand the potential of Fe-EC to treat chemical and microbial contamination concurrently.

Two processes in the Fe-EC system may contribute to microbe attenuation. The first process is the production of Fe(III) precipitates with an affinity for the surface of microorganisms, leading to their encapsulation in flocs and physical removal by settling. In many natural environments, Fe oxides are found in close association with bacterial cells or exopolymers[17–19], which suggests strong sorption affinities and has prompted the use of Fe oxides to remove bacteria[20–22] and viruses[23,24] in engineered systems. The second process is the transient presence of Fe(II) that can lead to oxidative stress and inactivation. Fe(II) oxidation in Fenton-type reactions produces strong oxidants (Fe(IV), $OH^{\cdot}$) that can inactivate bacteria[25] and viruses[26]. The processes leading to both physical removal with flocs and inactivation are largely governed by electrolyte composition, which can impact the phase, size and surface charge of EC precipitates[27,28], the rate of Fe(II) oxidation[29] and the lifetime of strong oxidants (HCO_3^-, Cl^-, As(III) and natural organic matter can quench Fe(IV) and $OH^{\cdot}$). Although some Fe-EC research has focused on microbe attenuation, the electrolytes used in these studies were designed to replicate contaminated surface water[24,30]. Therefore, the extent and mechanism of microbe attenuation by Fe-EC in electrolytes representative of Bengal groundwater, which is richer in oxyanions and bivalent cations than surface water, remain unexplored.

In addition to electrolyte composition, solution pH is likely to be a key factor affecting Fe-EC performance because it controls (1) the rate of Fe(II) oxidation[29] and thereby the residence time of potentially germicidal Fe(II) as well as the rate at which Fe(III) precipitates are generated, and (2) the surface charge of Fe(III) precipitates and

Published in Environmental Sci. and Technology (ACS), July 2015.
DOI:10.1021/acs.est.5b01696

their electrostatic interactions with microorganisms. Because the pH of arsenic-contaminated groundwater (defined as [As] > 10 µg/L) in Bengal varies between 6.4 and 8.4[31], it is essential to understand the effect of pH on microbe attenuation. Furthermore, since pH controls processes potentially leading to removal and inactivation, varying solution pH can help unravel the mechanisms of microbe attenuation in Fe-EC systems.

Natural organic matter (NOM) is present at non-negligible concentrations in arsenic-contaminated groundwater in Bengal (1-5 mg/L-C)[31,32] and may interfere with microbe attenuation by Fe-EC in several ways: quenching of strong oxidants, complexation of dissolved Fe(II)/Fe(III)[33], and alteration of the surface characteristics of Fe(III) precipitates and microorganisms. NOM is known to inhibit microbe-mineral interactions by increasing electrostatic repulsion[34,35], and has been shown to reduce the effectiveness of Fe-based microbe reduction processes[20,24,35]. It is therefore important to determine the impact of NOM on *E. coli* attenuation with Fe-EC.

The goals of this study were to: (1) examine the concurrent removal of arsenic and bacteria by Fe-EC in synthetic Bengal groundwater; (2) investigate the effects of pH and NOM on this process; and (3) determine the mechanism of bacteria attenuation. Using *Escherichia coli K12* as a model for gram-negative fecal bacteria, we first demonstrate 4-log bacteria attenuation by Fe-EC concurrent with arsenic removal from 450 μg/L to below 10 μg/L. Next we investigate the pH-dependence of *E. coli* attenuation in Fe-EC by (1) comparing Fe-EC with Fe chemical coagulation methods, (2) analyzing zetapotential measurements of EC precipitates and *E. coli*, and (3) varying Fe-EC operating parameters such as iron dosage rate and settling time. We combine these results with live-dead staining and transmission electron microscopy images to propose a

Published in Environmental Sci. and Technology (ACS), July 2015.
DOI:10.1021/acs.est.5b01696

mechanism for *E. coli* attenuation. Lastly, we discuss the effect of NOM on *E. coli* reduction by Fe-EC. Our results provide insight into the applicability of Fe-EC for concurrent arsenic and bacteria attenuation in contaminated Bengal groundwater.

2. Methods

2.1 Synthetic Bengal Groundwater Preparation. The procedure to prepare synthetic groundwater (SGW) was similar to Roberts et al[36] (see the Supporting Information for details). Concentrations of HCO_3^-, Ca^{2+} and Mg^{2+} (8.2 mM, 2.6 mM and 1.9 mM respectively) reflected average levels in arsenic-contaminated (defined as [As] > 10 μg/L) Bangladesh tubewells according to the British Geological Survey (BGS)[31]. Si, P and As concentrations (1.3 mM, 0.16 mM and 6.1 μM (460 μg/L) respectively) were significantly higher in SGW than average levels to represent worst-case scenarios for arsenic removal (Table S1). The target pH value (6.6 or 7.5) was maintained throughout experiments by adding drops of 1.1 M HCl as needed. Concentrations of As, Ca, Mg, P and Si were measured by inductively coupled plasma optical emission spectrometry (ICP-OES, PerkinElmer 5300 DV, measurement error typically < 5%). Initial concentrations of all ions varied by less than 10% in replicate batch experiments. ICP-OES with hydride generation was used to measure low (<20 μg/L) final As concentrations. For NOM experiments, 3 mg/L-C of Suwanee River Fulvic Acid (International Humic Substance Society) was added to SGW. The concentration of NOM was measured with a TOC-V analyzer (Shimadzu).

Published in Environmental Sci. and Technology (ACS), July 2015.
DOI:10.1021/acs.est.5b01696

2.2 *E. coli* Preparation and Enumeration. We used a non-pathogenic and kanamycin-resistant strain of the gram-negative bacterium *Escherichia coli* (NCM 4236) obtained from the late Dr. Sydney Kustu (UC Berkeley). After three propagations in kanamycin-amended tryptic soy broth, stationary-phase *E. coli* was rinsed and resuspended in phosphate buffer (see the Supporting Information for details). *E. coli* was spiked in SGW to achieve initial concentrations of $10^{6.1}$-$10^{6.7}$ CFU/mL. *E. coli* concentrations were enumerated in duplicate in 100 μL aliquots as colony forming units (CFU) using the spread plate technique on agar with 0.025 g/L kanamycin.

2.3 Electrocoagulation Experiments. All glassware was washed in 10% HNO_3, rinsed with 18 MΩ deionized water and autoclaved prior to use. Electrocoagulation experiments were conducted by immersing two 1cm x 8cm Fe(0) electrodes (98% Fe, 0.5 mm thick, 0.5 cm apart, anodic submerged area of 3 cm^2) in 200 mL SGW spiked with *E. coli*. Electrodes were cleaned with sand paper before each experiment to remove any rust or solid deposits. Within the tested current density range (0.3 to 10 mA/cm^2), the Fe dosage rate D (M Fe/s) is related to the applied current i (A or Coulombs/s) according to Faraday's law:

$$D = \frac{i}{V * Z * F}$$

where V is the reactor volume (L), Z is the number of electrons involved (equivalents/mol) and F is Faraday's constant (Coulombs/mol). We assume Z=2 based on Lakshmanan et al.[37]. Unless specified otherwise, an Fe dosage rate of 46.4 μM/min was selected (applied current of 30 mA) and the dosage time was adjusted to reach the desired final Fe concentration (varying from 0.1 to 2.5 mM). After dosing, the solution was stirred in

163 open air for 90 to 120 min to allow for Fe(II) oxidation and formation of Fe(III)
164 precipitates (these stages are referred to as "dosing-mixing" hereafter). The suspension
165 was then left to settle overnight. Unfiltered and filtered (0.45 μm nylon filters) samples
166 were taken before dosing, after dosing-mixing and after overnight settling for
167 measurement of Fe, As, Ca, Mg, P and Si with ICP-OES. All samples were digested with
168 1.1 M HCl prior to ICP-OES analysis. Unfiltered samples were used to measure total Fe
169 (Fe(II) + Fe(III)). Because Fe(III) is insoluble at circumneutral pH, Fe in filtered samples
170 was considered to be Fe(II). Across all experiments, unfiltered Fe in bulk solution after
171 dosing was 95% ± 7% (n=69) of the Faradic value. Fe in the filtrate (soluble Fe(II)) after
172 dosing-mixing was <0.1% of the total Fe dosed for experiments at pH 7.5, and 19% ± 6%,
173 (n=18) of the total Fe dosed for experiments at pH 6.6. Although complete (99.9%)
174 oxidation of Fe(II) in our SGW at pH 6.6 requires over 9h (see Figure S1), we chose not
175 to prolong mixing beyond 120 min to remain representative of field conditions. Fe
176 concentrations in the supernatant after overnight settling were typically <5% of the total
177 dosed Fe. Samples for *E. coli* enumeration were taken before dosing and after settling
178 (from the supernatant, ~ 3 cm below the surface). *E. coli* attenuation was calculated as the
179 difference between CFU concentrations in the pre-dosing and post-settling samples.
180 Overnight settling allowed separating individual *E. coli* cells from cells associated with
181 Fe(III) precipitates, because individual cells do not settle in this time frame (Stokes
182 settling velocity of 1 μm particles with a density of 1.16 g/cm^3[38] is about 1 cm/day). This
183 assumption was verified in preliminary experiments, which showed that: (1)
184 concentrations of *E. coli* cells suspended in SGW did not change after two days (less than

Published in Environmental Sci. and Technology (ACS), July 2015.
DOI:10.1021/acs.est.5b01696

4.5% change), and (2) *E. coli* CFUs at different depths in the supernatant in EC experiments varied by less than 0.2 log.

2.4 Fe-EC Experiments with Alum. To isolate the effects of removal and inactivation on *E.coli* attenuation during the settling period, several experiments were conducted with $Al_2(SO_4)_3$ coagulant (alum), which made it possible to decrease the time needed for settling of EC precipitates and quickly separate cells associated with flocs from free cells in the supernatant. After dosing-mixing, 0.1 mL of a 370 mM alum solution was added to the suspension, resulting in an Al concentration of 0.19 mM. After rapid mixing (700 rpm, 2 min) and slow mixing (60 rpm, 20 min), large flocs formed that settled in approximately 2h, as opposed to 18h in regular EC experiments (until Fe(III) in supernatant < 5% of total Fe dosed), allowing us to sample bacteria in the supernatant after 2h, 5h and 24h for culturability testing.

2.5 *E. coli* Attenuation by Coagulation with $FeSO_4$, $FeCl_3$ and Pre-Synthesized Ferrihydrite. Stock solutions of $FeSO_4$ (100 mM, acidified with 1 mM HCl to avoid premature Fe(II) oxidation), $FeCl_3$ (100 mM) and pre-synthesized ferrihydrite (200 mM, see the Supporting Information for details) were prepared. Adequate volumes of these stock solutions were added to 200 mL SGW adjusted to pH 6.6 or 7.5 to achieve Fe concentrations of 0.5 mM. Solutions were stirred open to the atmosphere for 100-130 min, then left to settle overnight. Sampling followed the same procedure as in EC experiments.

Published in Environmental Sci. and Technology (ACS), July 2015.
DOI:10.1021/acs.est.5b01696

2.6 *E. coli* Attenuation at Varying Generation Rates of Fe(III) Precipitates. In Fe-EC, the rate at which Fe(III) precipitates are generated is controlled by two processes: (1) Fe(II) production at the anode, and (2) Fe(II) oxidation to Fe(III), which instantaneously (relative to Fe(II) oxidation) precipitates at circumneutral pH. A detailed derivation of the generation rate of Fe(III) precipitates is given in the Supporting Information. At pH 7.5, Fe(II) oxidation is rapid ($t_{1/2}$ = 4.5 min in SGW, see Figure S1b) and the generation rate of precipitates is mainly controlled by the Fe dosage rate. In order to investigate the impact of the generation rate of Fe(III) precipitates on *E. coli* attenuation, Fe-EC experiments were conducted at pH 7.5 at three different Fe dosage rates (1.1, 2.6 and 46.4 μM/min, corresponding to currents of 1, 2 and 30 mA respectively) and three different total dosages (0.1, 0.2 and 0.5 mM respectively, see Figure S2). One experiment was carried out with $FeCl_3$ at pH 7.5 where 6 μL of 100 mM $FeCl_3$ were added to the reaction beaker every minute in order to mimic a dosage rate of 3.1 μM/min. A reaction time (dosing-mixing) of 100 min was kept constant across all experiments.

All *E. coli* attenuation experiments were conducted in triplicate or more. We report average log attenuations ± one standard deviation.

2.7 Bacterial Viability Tests. Quantifying *E. coli* inactivation by direct plating would require enumerating viable cells in the supernatant as well as in the settled flocs. However, separating *E. coli* from Fe(III) precipitates was not possible here (see the Supporting Information for details). Instead, we used the BacLight LIVE-DEAD kit (Invitrogen) to assess the degree of membrane permeabilization, a proxy for *E. coli*

inactivation. This test relies on two fluorescent nucleic acid stains (PI and SYTO9) to distinguish cells with intact membranes appearing green ("live") from those with damaged membranes appearing red ("dead"). Samples were prepared as described in the Supporting Information and analyzed with a Zeiss AxioImager fluorescent microscope (63x Plan-Apochromat objective, EndoGFP and mCherry filters, UC Berkeley CNR Biological Imaging Facility). Pictures of Fe(III) precipitates and stained *E. coli* cells were taken in transmission and fluorescent modes respectively, and images were superimposed. At least 10 pictures were taken per sample and visually analyzed to produce representative results.

We applied this procedure to evaluate *E. coli* inactivation during the two treatment stages: dosing-mixing and overnight settling. For the former, samples were collected from the mixed suspension at the end of dosing-mixing in EC experiments (at pH 6.6 and 7.5). For the latter, sampling the supernatant after settling did not allow for quantitative fluorescent microscopy analysis because *E. coli* concentrations were too low. We therefore mimicked supernatant conditions at pH 6.6 with 200 mL solutions of SGW amended with 0.18 mM $FeSO_4$ and spiked with $10^{7.5}$ CFU/mL *E. coli*.

2.8 Bacteria and Precipitates Characterization. Transmission electron microscopy was carried out on the precipitate-microorganism aggregates with a FEI Tecnai 12 Transmission Electron Microscope operated at 120 kV (UC Berkeley Electron Microscope Lab). Zetapotential measurements were conducted with a Malvern Zetasizer Nano-ZS at 633 nm for (1) Fe(III) precipitates generated by Fe-EC in SGW with and without NOM (Fe dosage = 0.5 mM) and (2) *E. coli* suspended in SGW ($10^{6.5}$ CFU/mL).

Published in Environmental Sci. and Technology (ACS), July 2015.
DOI:10.1021/acs.est.5b01696

Sample preparation and data collection are described in detail in the Supporting Information.

3. Results and discussion

3.1 Concurrent As and *E. coli* Attenuation. Figure 1 shows concurrent As and *E. coli* attenuation in SGW at pH 7.5. For Fe dosages of 0.5, 1.5 and 2.5 mM, Fe-EC achieved log attenuations of 1.9, 3.7 and 4.4 respectively. Arsenic was reduced from 450 μg/L to 116 μg/L at 0.5 mM Fe, and to below the WHO recommended maximum contaminant level (MCL) of 10 μg/L[39] at Fe dosages > 1.5 mM. Similar arsenic removal in SGW with and without *E. coli* (Table S2) suggests that Fe-EC can attenuate bacteria without detriment to arsenic remediation. At Fe dosages of more than 2 mM, which are typical of current field operation[16], Fe-EC achieved over 4-log attenuation of *E. coli* and thus met the WHO guideline for household drinking water treatment requiring 4-log bacteria reduction[40]. This level of treatment is likely sufficient to eliminate the need for an additional disinfection step for most groundwaters as WHO drinking water guidelines characterize waters as low risk if *E. coli* < 1 CFU/100 mL[39].

3.2 Surface Charge Characterization of EC precipitates and *E. coli*. Figure 2 shows the zetapotentials of EC precipitates and *E. coli* in SGW between pH 1.5 and 8.5. The isoelectric point (iep) of *E. coli* was found to be between 2 and 3, which is consistent with reported iep of gram-negative bacteria[41]. Above pH 5, the zetapotential of *E. coli* cells was less negative than that observed previously in a KCl electrolyte[42], which could be due to Ca^{2+} and Mg^{2+} complexation by negatively charged residues on the cell

277 surface[43]. Past studies have shown that Fe-EC in SGW leads to the formation of short-
278 range ordered hydrous ferric oxide[14,27]. We found the iep of EC precipitates to be between
279 4 and 5, which is lower than iep values typically reported for poorly ordered Fe(III)
280 precipitates (between 6 and 9)[44,45]. This difference can be attributed to the adsorption of
281 silicate and negatively charged phosphate (Si:Fe and P:Fe of 0.028±0.08 and 0.24±0.02
282 mol:mol, n=7), which are known to decrease the iep of ferrihydrite upon adsorption[45,46].
283 Our zetapotential measurements indicate that EC precipitates and *E. coli* are both
284 negatively charged at circumneutral pH in SGW, and that their surface charge does not
285 significantly vary between pH 5.5 and 8.5.

286

287 **3.3 Effect of pH on *E. coli* Attenuation.** In Figure 3, *E. coli* attenuation at pH 6.6
288 and 7.5 is compared for 4 different scenarios (Fe-EC, chemical coagulation with ferrous
289 and ferric salts, and coagulation with pre-synthesized ferrihydrite) at an Fe dosage of 0.5
290 mM. These 4 scenarios have been shown to generate the same type of precipitates[14,36,47,48]
291 and only differ by the form and rate with which Fe is released into SGW: as Fe(II) for Fe-
292 EC and $FeSO_4$ (released progressively and in a single dose respectively), as dissolved
293 Fe(III) for $FeCl_3$, and as colloidal Fe(III) for pre-synthesized ferrihydrite (both released in
294 a single dose). With Fe-EC, *E. coli* attenuation was significantly higher at lower pH: 4.0
295 log removal at pH 6.6 compared to 1.9 at pH 7.5. A similar trend was observed for $FeSO_4$
296 (4.3 log at pH 6.6 and 2.0 log at pH 7.5). Conversely, pH had no significant effect on *E.*
297 *coli* attenuation with $FeCl_3$ and with pre-synthesized ferrihydrite, indicating that possible
298 changes in colloid surface charge or SGW chemistry between pH 6.6 and 7.5 have no
299 impact on bacteria-precipitate surface interactions. Consequently, the increased *E. coli*

Published in Environmental Sci. and Technology (ACS), July 2015.
DOI:10.1021/acs.est.5b01696

reduction with Fe-EC and $FeSO_4$ at pH 6.6 cannot be attributed to a difference in colloid surface charge, which is supported by our zetapotential measurements showing that both EC precipitates and *E. coli* cells have nearly identical net surface charge at pH 6.6 and 7.5 (zetapotential ~ -12.0 mV and -13.4 mV respectively, Figure 2).

E. coli attenuation with $FeSO_4$ exhibited the same pH dependence as Fe-EC, suggesting that increased attenuation at lower pH is related to the transient presence of Fe(II). The rate of Fe(II) oxidation in SGW at pH 6.6 (k_{eff} = 0.012 min^{-1}, Figure S1) is significantly slower than at pH 7.5 (k_{eff} = 0.155 min^{-1}, Figure S1), which leads to: (1) a slower generation rate of Fe(III) precipitates, and (2) an increased residence time of germicidal Fe(II). In the two following sections, we investigate the impacts of these two factors on *E. coli* attenuation by Fe-EC.

3.4 Effect of the Generation Rate of Fe(III) Precipitates on *E. coli* Attenuation.

The generation rate of Fe(III) precipitates controls the rate at which they aggregate into flocs, and may thus affect bacteria-precipitate interactions. To probe the impact of the precipitate generation rate on *E. coli* attenuation, the Fe dosage rate q, which controls the flux of Fe(II) delivered by the anode, was decreased from 46.4 to 2.6 and 1.1 μM/min at pH 7.5. As calculated by Equations (5) and (6) of the Supporting Information, q = 2.6 μM/min at pH 7.5 leads to a precipitate generation rate comparable to that of experiments at pH 6.6 with q = 46.4 μM/min (see Figure S2). Figure S3 shows that lower dosage rates, resulting in lower precipitate generation rates, did not significantly improve *E. coli* attenuation by Fe-EC at pH 7.5. Similarly, no significant difference in *E. coli* attenuation was observed between single dose versus low dosage rate

for chemical coagulation with $FeCl_3$ at pH 7.5. We concluded that the lower precipitate generation rate at pH 6.6 cannot account for increased *E. coli* attenuation compared to pH 7.5.

3.5 Evolution of *E. coli* Attenuation during Settling in Experiments with Alum.

The use of alum in EC experiments significantly accelerated settling of Fe(III) precipitates and allowed us to quickly separate *E. coli* cells associated with precipitates from free cells in the supernatant. As a result, this experimental design enabled us to track the viability of suspended *E. coli* cells in the supernatant during the 24h settling period. We found that the difference in *E. coli* attenuation between pH 6.6 and pH 7.5 increased over the 24h settling period (Figure 4). After 2h settling, *E. coli* attenuation was only slightly higher at pH 6.6 compared to pH 7.5 (2.5 and 1.8 log respectively). The discrepancy significantly increased over time and was comparable to that of regular EC experiments after 24h settling (5.0 and 2.5 log attenuation at pH 6.6 and 7.5 with alum, compared to 4.0 and 1.9 log attenuation at pH 6.6 and 7.5 in regular EC experiments). In contrast to experiments at pH 7.5, those at pH 6.6 contained a significant concentration of unoxidized Fe(II) at the beginning of settling (0.10 ± 0.04 mM, corresponding to 19% ± 6% of the total Fe dosed, n=9), most of which oxidized during the 24h settling period. Figure 4 shows a correlation at pH 6.6 between the increase of *E. coli* attenuation during overnight settling and the amount of Fe(II) oxidized in the supernatant. This correlation could point to the bactericidal action of Fe(II) on *E. coli* in the supernatant. To further investigate this possibility, we conducted live-dead staining of the bacteria.

Published in Environmental Sci. and Technology (ACS), July 2015.
DOI:10.1021/acs.est.5b01696

346 **3.6 *E. coli* Inactivation.** Bacterial viability tests conducted immediately after
347 dosing-mixing showed that *E. coli* inactivation during dosing-mixing was limited, both at
348 pH 6.6 and 7.5, with less than 20% of the cells appearing red on fluorescent microscopy
349 images (representative examples shown in Figure 5a-c). Bacterial viability tests on the
350 supernatant after overnight settling at pH 6.6 showed a majority of red cells (see Figure
351 S4), suggesting *E. coli* inactivation during the settling period at pH 6.6. However, *E. coli*
352 concentrations in the supernatant were too low for quantitative fluorescent microscopy
353 analysis. Thus, we mimicked supernatant conditions at pH 6.6 by adding $10^{7.5}$ CFU/mL
354 and 0.18 mM $FeSO_4$ to SGW. In images taken after 18h, approximately 50% of the cells
355 appeared red (Figure 5d), suggesting that reactive species produced upon Fe(II) oxidation
356 in the supernatant at pH 6.6 caused significant membrane damage (confirmed by
357 culturability measurements indicating a 0.8 log reduction in CFUs).
358
359 **3.7 Mechanism of *E. coli* attenuation by Fe-EC.** At pH 7.5, all Fe(II) is
360 oxidized by the end of dosing-mixing. Consequently, minimal inactivation at the end of
361 dosing-mixing (<0.1 log as determined on fluorescent microscopy images, Figure 5a)
362 implies that inactivation is overall insignificant and that *E. coli* attenuation is primarily
363 due to physical removal with flocs by gravitational settling. As shown on Figure 3, *E. coli*
364 reduction at pH 7.5 with Fe-EC is not significantly different from the attenuation
365 achieved with $FeCl_3$ (pH 6.6 or 7.5). The latter only removes *E. coli* via encapsulation in
366 flocs, since inactivation by germicidal Fe(II) can be ruled out in the case of a ferric salt.
367 Consequently, similar *E. coli* reduction with Fe-EC at pH 7.5 and with $FeCl_3$ further

supports that removal with flocs is the primary mechanism of *E. coli* attenuation by Fe-EC at pH 7.5.

By contrast, our results suggest that both removal and inactivation contribute to *E. coli* reduction at pH 6.6. Inactivation after dosing-mixing at pH 6.6 was insignificant (<0.1 log as determined from fluorescent microscopy images, Figure 5b-c), suggesting that the attenuation observed at the earliest stage of settling (2.5 log after 2h, Figure 4) is mostly due to removal with flocs. The additional ~2 log attenuation occurring in the supernatant during overnight settling is likely attributable to inactivation, supported by the increase in dead cells in the supernatant (Figure S4) and mock supernatant (Figure 5d). Note that the live-dead stain is likely a conservative measure of inactivation, as loss of viability may occur well before membranes become permeable to PI[49]. In addition, the higher bacteria concentration in the mock supernatant compared to regular supernatant conditions could have lowered the steady-state concentration of reactive oxidants through scavenging, explaining the limited inactivation (0.8-log loss of culturability) in the mock supernatant.

We established that the largest fraction of *E. coli* cells (1.9 log at pH 7.5, ~2 log at pH 6.6, Figures 3 and 4) is physically removed with flocs. Figures 5a-b illustrate the association of *E. coli* cells with large Fe(III) flocs. TEM images provide further insight, illustrating the intimate spatial arrangement between EC precipitates and bacteria surfaces (Figures 6 and S5a). Precipitates bridging individual cells (Figure 6) lead to large precipitate-bacteria networks that can be readily removed by gravitational settling (Figure S5b). Although our zetapotential measurements indicate that EC precipitates and *E. coli* are both negatively charged at circumneutral pH in SGW (Figure 2), adhesion of

Published in Environmental Sci. and Technology (ACS), July 2015.
DOI:10.1021/acs.est.5b01696

EC precipitates to *E. coli* may be enabled by a combination of 1) charge heterogeneities on cell surfaces, 2) hydrophobic interactions, and 3) hydrogen or covalent bonds. Due to their small size relative to *E. coli* cells (apparent in Figure 6), EC precipitates may be sensitive to heterogeneities in *E. coli* surface composition, allowing localized adhesion. For example, surface proteins carrying positively charged amine groups could constitute preferential adhesion sites. In addition, phosphate and carboxyl residues, which can form covalent bonds with iron oxides[50], may provide chemical bonding sites for Fe(III) precipitates.

3.8 Effect of NOM on *E. coli* Attenuation. 3 mg/L-C of Suwanee River Fulvic Acid had a minimal impact on *E. coli* attenuation both at pH 6.6 (0.5 mM Fe) and 7.5 (1.5 mM Fe), as illustrated on Figure S6a. The zetapotential of EC precipitates, shown in Figure S6b, was not affected by NOM between pH 5.5 and 8.5. ICP-OES analysis of filtered samples after dosing-mixing indicated that Ca^{2+}/Mg^{2+} uptake did not increase in the presence of NOM (data not shown), ruling out bivalent cation bridging of EC precipitates and NOM. Taken together, these results suggest that NOM did not significantly interact with EC precipitates, and therefore did not interfere with the adhesion of EC precipitates to *E. coli* cells.

These results are unexpected given the accounts of NOM adsorbing to ferric (oxyhydr)oxides[34,51] and inhibiting MS2 attenuation by Fe-EC in a $CaCl_2$ electrolyte[24], but may be explained by the composition of SGW. NOM may not effectively compete with silicate and phosphate for surface sites on EC precipitates: decreased NOM adsorption on Fe oxides in the presence of silicate and phosphate has been observed elsewhere[52,53]. In

addition, EC precipitates have a net negative charge in SGW, and electrostatic repulsion may inhibit interactions with NOM. Conversely, EC precipitates formed in $CaCl_2$ are expected to be positively charged at circumneutral pH and more prone to interact with NOM, likely explaining the results of Tanneru and Chellam[24]. In their paper, they also proposed that quenching of $OH^{\cdot}$ and Fe(IV) by NOM may inhibit inactivation of MS2[24]. In our system, 3 mg/L-C of NOM did not have a significant effect on overall attenuation at pH 6.6, possibly because NOM concentrations were lower (C:Fe mass ratios of 0.03-0.1 in our experiments, compared to 0.5 in Tanneru and Chellam[24]). It is possible that higher NOM concentrations would cause a larger decrease in *E. coli* attenuation at pH 6.6 due to greater quenching of reactive oxidants.

3.9 Implications for Water Treatment. In this work, we show that Fe-EC can adequately reduce bacterial contamination from synthetic Bengal groundwater, even in the presence of 3 mg/L-C NOM, and without detriment to arsenic removal. Groundwater remediation with Fe-EC in arsenic-affected areas may therefore not need to be followed by chlorination or UV disinfection. However, more research on virus attenuation by Fe-EC is needed to reinforce this claim. Because bacterial inactivation during dosing-mixing was limited, settled flocs may contain viable pathogens, presenting a risk if sludge is not handled properly. Consequently, adequate sludge treatment such as high-temperature drying (70 C for 30 min[54]) should be applied to ensure sludge sterilization. Finally, we found that the longer lifetime of Fe(II) at lower pH led to increased attenuation, suggesting that the use of ferrous salts (as opposed to ferric salts) in primary water and wastewater treatment might improve microbe reduction when the pH of the influent is

437 acidic. More generally, our results suggest that conditions promoting Fe(II) build-up in
438 the Fe-EC process, such as a low pH, a short post-EC mixing time, or a very high dosage
439 rate causing O_2 depletion, may lead to increased bacteria reduction.

440

441 **Supporting Information**

442 Detailed methodology and supporting figures referenced in the text are provided in the
443 Supporting Information. This material is available free of charge via the Internet at
444 http://pubs.acs.org.

445

446 **Acknowledgements**

447 This work was supported by the Development Impact Lab (USAID Cooperative
448 Agreement AID-OAA-A-13-00002), part of the USAID Higher Education Solutions
449 Network, and by the Andrew and Virginia Rudd Family Foundation. This work would
450 not have been possible without the generous assistance from David Sedlak, Andrew
451 Torkelson, Andrea Silverman, Samantha Beardsley, Jannis Wenk, Denise Schichnes and
452 Reena Zalpouri. We are grateful to James Britt Abrahamson for conducting zetapotential
453 measurements. We thank the CNR Biological Imaging Facility and the Electron
454 Microscope Lab at UC Berkeley. Work at the Molecular Foundry (zetapotential
455 measurements) was supported by the Office of Basic Energy Sciences of the U.S.
456 Department of Energy under Contract No. DE-AC02-05CH11231.

457

458

459

Published in Environmental Sci. and Technology (ACS), July 2015.
DOI:10.1021/acs.est.5b01696

References

(1) Rahman, M. M.; Naidu, R.; Bhattacharya, P. Arsenic contamination in groundwater in the Southeast Asia region. *Environ. Geochem. Health* **2009**, *31 Suppl 1*, 9–21.

(2) Van Geen, A.; Ahmed, K. M.; Akita, Y.; Alam, M. J.; Culligan, P. J.; Emch, M.; Escamilla, V.; Feighery, J.; Ferguson, A. S.; Knappett, P.; et al. Fecal contamination of shallow tubewells in bangladesh inversely related to arsenic. *Environ. Sci. Technol.* **2011**, *45*, 1199–1205.

(3) Ferguson, A. S.; Layton, A. C.; Mailloux, B. J.; Culligan, P. J.; Williams, D. E.; Smartt, A. E.; Sayler, G. S.; Feighery, J.; McKay, L. D.; Knappett, P. S. K.; et al. Comparison of fecal indicators with pathogenic bacteria and rotavirus in groundwater. *Sci. Total Environ.* **2012**, *431*, 314–322.

(4) Knappett, P. S. K.; McKay, L. D.; Layton, A.; Williams, D. E.; Alam, M. J.; Mailloux, B. J.; Ferguson, A. S.; Culligan, P. J.; Serre, M. L.; Emch, M.; et al. Unsealed tubewells lead to increased fecal contamination of drinking water. *J. Water Health* **2012**, *10*, 565–578.

(5) Leber, J.; Rahman, M. M.; Ahmed, K. M.; Mailloux, B.; van Geen, A. Contrasting influence of geology on E. coli and arsenic in aquifers of Bangladesh. *Ground Water 49*, 111–123.

(6) Islam, M. S.; Siddika, A.; Khan, M. N.; Goldar, M. M.; Sadique, M. A.; Kabir, A. N.; Huq, A.; Colwell, R. R. Microbiological analysis of tube-well water in a rural area of Bangladesh. *Appl. Environ. Microbiol.* **2001**, *67*, 3328–3330.

(7) Luby, S. P.; Gupta, S. K.; Sheikh, M. A.; Johnston, R. B.; Ram, P. K.; Islam, M. S. Tubewell water quality and predictors of contamination in three flood-prone areas in Bangladesh. *J. Appl. Microbiol.* **2008**, *105*, 1002–1008.

(8) Hira-Smith, M. M.; Yuan, Y.; Savarimuthu, X.; Liaw, J.; Hira, A.; Green, C.; Hore, T.; Chakraborty, P.; von Ehrenstein, O. S.; Smith, A. H. Arsenic concentrations and bacterial contamination in a pilot shallow dugwell program in West Bengal, India. *J. Environ. Sci. Health. A. Tox. Hazard. Subst. Environ. Eng.* **2007**, *42*, 89–95.

(9) Sengupta, C.; Sukumaran, D.; Barui, D.; Saha, R.; Chattopadhyay, A.; Naskar, A.; Dave, S. Water Health Status in Lower Reaches of River Ganga, India. *Appl. Ecol. Environ. Sci.* **2014**, *2*, 20–24.

(10) Escamilla, V.; Knappett, P. S. K.; Yunus, M.; Streatfield, P. K.; Emch, M. Influence of Latrine Proximity and Type on Tubewell Water Quality and Diarrheal Disease in Bangladesh. *Ann. Assoc. Am. Geogr.* **2013**, *103*, 299–308.

(11) Wu, J.; van Geen, A.; Ahmed, K. M.; Alam, Y. A. J.; Culligan, P. J.; Escamilla, V.; Feighery, J.; Ferguson, A. S.; Knappett, P.; Mailloux, B. J.; et al. Increase in diarrheal disease associated with arsenic mitigation in Bangladesh. *PLoS One* **2011**, *6*, e29593.

(12) Amrose, S.; Gadgil, A.; Srinivasan, V.; Kowolik, K.; Muller, M.; Huang, J.; Kostecki, R. Arsenic removal from groundwater using iron electrocoagulation: effect of charge dosage rate. *J. Environ. Sci. Health. A. Tox. Hazard. Subst. Environ. Eng.* **2013**, *48*, 1019–1030.

(13) Amrose, S. E.; Bandaru, S. R. S.; Delaire, C.; van Genuchten, C. M.; Dutta, A.; DebSarkar, A.; Orr, C.; Roy, J.; Das, A.; Gadgil, A. J. Electro-chemical arsenic remediation: field trials in West Bengal. *Sci. Total Environ.* **2014**, *488-489*, 539–546.

(14) Van Genuchten, C. M.; Addy, S. E. A.; Peña, J.; Gadgil, A. J. Removing arsenic from synthetic groundwater with iron electrocoagulation: an Fe and As K-edge EXAFS study. *Environ. Sci. Technol.* **2012**, *46*, 986–994.

(15) Li, L.; van Genuchten, C. M.; Addy, S. E. A.; Yao, J.; Gao, N.; Gadgil, A. J. Modeling As(III) oxidation and removal with iron electrocoagulation in groundwater. *Environ. Sci. Technol.* **2012**, *46*, 12038–12045.

(16) Amrose, S. E.; Bandaru, S. R. S.; Delaire, C.; van Genuchten, C. M.; Dutta, A.; Debsarkar, A.; Orr, C.; Das, A.; Roy, J.; Gadgil, A. Electro-chemical arsenic remediation: field trials in West Bengal. *Sci. Total Environ.* **2013**, *in press*.

(17) Fortin, D.; Ferris, F. G. Precipitation of iron, silica, and sulfate on bacterial cell surfaces. *Geomicrobiol. J.* **1998**, *15*, 309–324.

(18) Ferris, F. G.; Beveridge, T. J.; Fyfe, W. S. Iron-silica crystallite nucleation by bacteria in a geothermal sediment. *Nature* **1986**, *320*, 609–611.

(19) Cowen, J. P.; Bruland, K. W. Metal deposits associated with bacteria: implications for Fe and Mn marine biogeochemistry. *Deep Sea Res. Part A. Oceanogr. Res. Pap.* **1985**, *32*, 253–272.

(20) Mohanty, S. K.; Torkelson, A. A.; Dodd, H.; Nelson, K. L.; Boehm, A. B. Engineering solutions to improve the removal of fecal indicator bacteria by bioinfiltration systems during intermittent flow of stormwater. *Environ. Sci. Technol.* **2013**, *47*, 10791–10798.

(21) Zhang, L.; Seagren, E. A.; Davis, A. P.; Karns, J. S. The capture and destruction of Escherichia coli from simulated urban runoff using conventional bioretention media and iron oxide-coated sand. *Water Environ. Res.* **2010**, *82*, 701–714.

(22) Zhuang, J.; Jin, Y. Interactions between viruses and goethite during saturated flow: effects of solution pH, carbonate, and phosphate. *J. Contam. Hydrol.* **2008**, *98*, 15–21.

(23) Zhu, B.; Clifford, D. A.; Chellam, S. Virus removal by iron coagulation–microfiltration. *Water Res.* **2005**, *39*, 5153–5161.

(24) Tanneru, C. T.; Chellam, S. Mechanisms of virus control during iron electrocoagulation--microfiltration of surface water. *Water Res.* **2012**, *46*, 2111–2120.

(25) Kim, J. Y.; Park, H.-J.; Lee, C.; Nelson, K. L.; Sedlak, D. L.; Yoon, J. Inactivation of Escherichia coli by nanoparticulate zerovalent iron and ferrous ion. *Appl. Environ. Microbiol.* **2010**, *76*, 7668–7670.

(26) Kim, J. Y.; Lee, C.; Love, D. C.; Sedlak, D. L.; Yoon, J.; Nelson, K. L. Inactivation of MS2 coliphage by ferrous ion and zero-valent iron nanoparticles. *Environ. Sci. Technol.* **2011**, *45*, 6978–6984.

(27) Van Genuchten, C. M.; Peña, J.; Amrose, S. E.; Gadgil, A. J. Structure of Fe(III) precipitates generated by the electrolytic dissolution of Fe(0) in the presence of groundwater ions. *Geochim. Cosmochim. Acta* **2014**, *127*, 285–304.

(28) Van Genuchten, C. M.; Gadgil, A. J.; Peña, J. Fe(III) nucleation in the presence of bivalent cations and oxyanions leads to subnanoscale 7 Å polymers. *Environ. Sci. Technol.* **2014**, *48*, 11828–11836.

(29) King, D. W. Role of Carbonate Speciation on the Oxidation Rate of Fe(II) in Aquatic Systems. *Environ. Sci. Technol.* **1998**, *32*, 2997–3003.

(30) Ghernaout, D.; Badis, A.; Kellil, A.; Ghernaout, B. Application of electrocoagulation in Escherichia coli culture and two surface waters. *Desalination* **2008**, *219*, 118–125.

(31) BGS. Arsenic contamination of groundwater in Bangladesh. *Arsen. Contam. Groundw. Bangladesh* **2001**.

(32) Tareq, S. M.; Maruo, M.; Ohta, K. Characteristics and role of groundwater dissolved organic matter on arsenic mobilization and poisoning in Bangladesh. *Phys. Chem. Earth, Parts A/B/C* **2013**, *58-60*, 77–84.

(33) Fujii, S.; Dupin, D.; Araki, T.; Armes, S. P.; Ade, H. First direct imaging of electrolyte-induced deswelling behavior of pH-responsive microgels in aqueous media using scanning transmission X-ray microscopy. *Langmuir* **2009**, *25*, 2588–2592.

(34) Abudalo, R. A.; Ryan, J. N.; Harvey, R. W.; Metge, D. W.; Landkamer, L. Influence of organic matter on the transport of Cryptosporidium parvum oocysts in a ferric oxyhydroxide-coated quartz sand saturated porous medium. *Water Res.* **2010**, *44*, 1104–1113.

(35) Li, Z.; Greden, K.; Alvarez, P. J. J.; Gregory, K. B.; Lowry, G. V. Adsorbed polymer and NOM limits adhesion and toxicity of nano scale zerovalent iron to E. coli. *Environ. Sci. Technol.* **2010**, *44*, 3462–3467.

(36) Roberts, L. C.; Hug, S. J.; Ruettimann, T.; Billah, M. M.; Khan, A. W.; Rahman, M. T. Arsenic Removal with Iron(II) and Iron(III) in Waters with High Silicate and Phosphate Concentrations. *Environ. Sci. Technol.* **2004**, *38*, 307–315.

(37) Lakshmanan, D.; Clifford, D. A.; Samanta, G. Ferrous and Ferric Ion Generation During Iron Electrocoagulation. *Environ. Sci. Technol.* **2009**, *43*, 3853–3859.

(38) Godin, M.; Bryan, A. K.; Burg, T. P.; Babcock, K.; Manalis, S. R. Measuring the mass, density, and size of particles and cells using a suspended microchannel resonator. *Appl. Phys. Lett.* **2007**, *91*, 123121.

(39) WHO | Guidelines for drinking-water quality, fourth edition. **2011**.

(40) WHO | Evaluating household water treatment options. **2011**.

(41) Rijnaarts, H. H. M.; Norde, W.; Lyklema, J.; Zehnder, A. J. B. The isoelectric point of bacteria as an indicator for the presence of cell surface polymers that inhibit adhesion. *Colloids Surfaces B Biointerfaces* **1995**, *4*, 191–197.

(42) Walker, S. L.; Redman, J. A.; Elimelech, M. Role of Cell Surface Lipopolysaccharides in Escherichia coli K12 adhesion and transport. *Langmuir* **2004**, *20*, 7736–7746.

(43) Fowle, D. A.; Fein, J. B. Competitive adsorption of metal cations onto two gram positive bacteria: testing the chemical equilibrium model. *Geochim. Cosmochim. Acta* **1999**, *63*, 3059–3067.

(44) Kosmulski, M. The pH-dependent surface charging and the points of zero charge. *J. Colloid Interface Sci.* **2002**, *253*, 77–87.

(45) Appenzeller, B. M. R.; Duval, Y. B.; Thomas, F.; Block, J.-C. Influence of Phosphate on Bacterial Adhesion onto Iron Oxyhydroxide in Drinking Water. *Environ. Sci. Technol.* **2002**, *36*, 646–652.

(46) Hamid, R. D.; Swedlund, P. J.; Song, Y.; Miskelly, G. M. Ionic strength effects on silicic acid (H4SiO4) sorption and oligomerization on an iron oxide surface: an interesting interplay between electrostatic and chemical forces. *Langmuir* **2011**, *27*, 12930–12937.

(47) Wan, W.; Pepping, T. J.; Banerji, T.; Chaudhari, S.; Giammar, D. E. Effects of water chemistry on arsenic removal from drinking water by electrocoagulation. *Water Res.* **2011**, *45*, 384–392.

(48) Li, L.; Li, J.; Shao, C.; Zhang, K.; Yu, S.; Gao, N.; Deng, Y.; Yin, D. Arsenic removal in synthetic ground water using iron electrolysis. *Sep. Purif. Technol.* **2014**, *122*, 225–230.

(49) Joux, F.; Lebaron, P. Use of fluorescent probes to assess physiological functions of bacteriaat single-cell level. *Microbes Infect.* **2000**, *2*, 1523–1535.

(50) Parikh, S. J.; Chorover, J. ATR-FTIR spectroscopy reveals bond formation during bacterial adhesion to iron oxide. *Langmuir* **2006**, *22*, 8492–8500.

(51) Gu, B.; Schmitt, J.; Chen, Z.; Liang, L.; McCarthy, J. F. Adsorption and desorption of natural organic matter on iron oxide: mechanisms and models. *Environ. Sci. Technol.* **1994**, *28*, 38–46.

(52) Giasuddin, A. B. M.; Kanel, S. R.; Choi, H. Adsorption of Humic Acid onto Nanoscale Zerovalent Iron and Its Effect on Arsenic Removal. *Environ. Sci. Technol.* **2007**, *41*, 2022–2027.

(53) Jiang, L.; Zhu, J.; Wang, H.; Fu, Q.; Hu, H.; Huang, Q.; Violante, A.; Huang, L. Sorption of humic acid on Fe oxides, bacteria, and Fe oxide-bacteria composites. *J. Soils Sediments* **2014**, *14*, 1378–1384.

(54) Feachem, R. G. *Bradley. D. J. *Garelick. H. D. D. Sanitation and disease□: health aspects of excreta and wastewater management. **1983**, 1–534.

Published in Environmental Sci. and Technology (ACS), July 2015.
DOI:10.1021/acs.est.5b01696

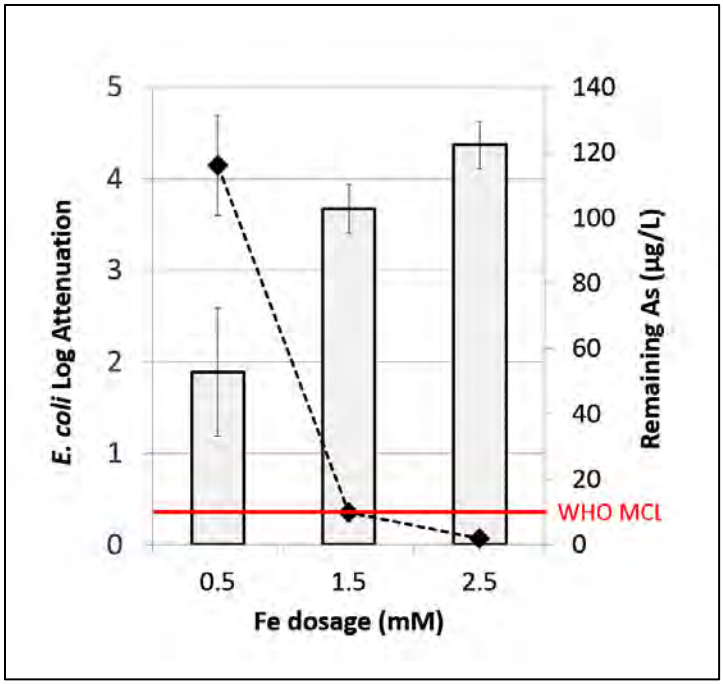

Figure 1: Concurrent As and *E. coli* attenuation by Fe-EC in SGW at pH 7.5 for Fe dosages of 0.5, 1.5 and 2.5 mM. The initial As concentration was 450 µg/L as As(III). The columns represent *E. coli* log attenuation, whereas the diamonds indicate dissolved arsenic concentrations. The solid red line indicates WHO recommended maximum contaminant level (MCL) for As, 10 µg/L.

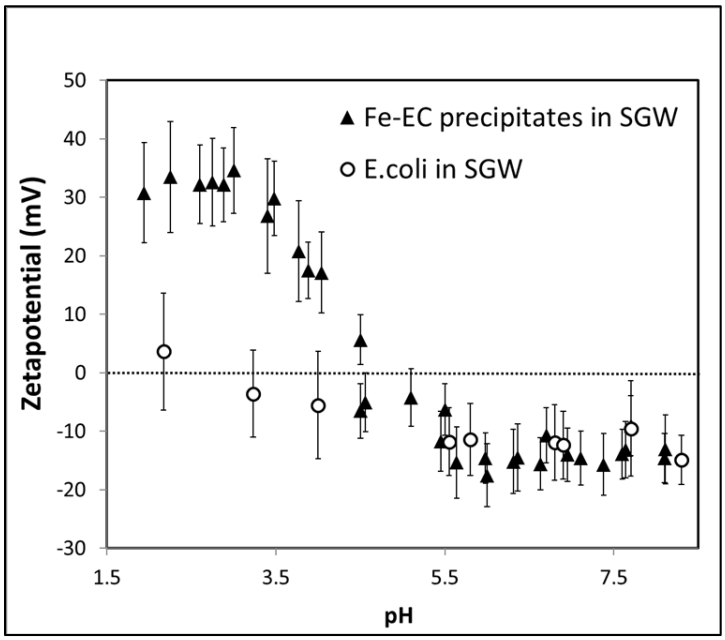

Figure 2: Zetapotential of Fe-EC precipitates (0.5 mM Fe) and *E. coli* in SGW measured by dynamic light scattering (633 nm).

Published in Environmental Sci. and Technology (ACS), July 2015.
DOI:10.1021/acs.est.5b01696

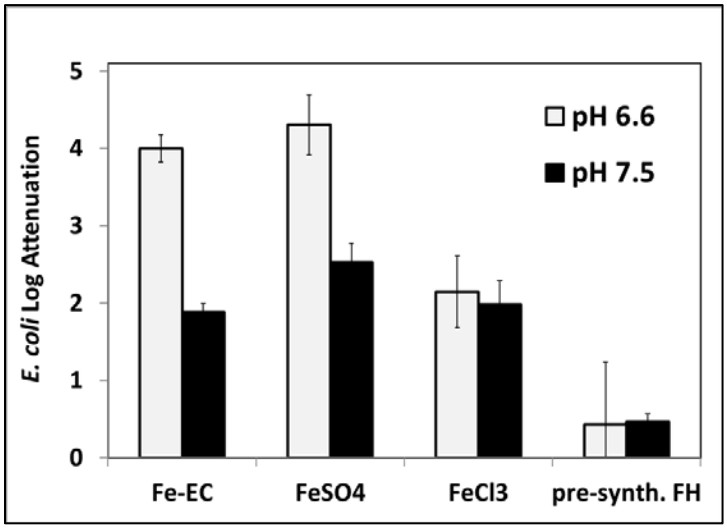

Figure 3: Effect of pH on *E. coli* attenuation by Fe-EC and chemical coagulation with $FeSO_4$ salt, $FeCl_3$ salt and pre-synthesized ferrihydrite (FH). The Fe dosage for all experiments was 0.5 mM.

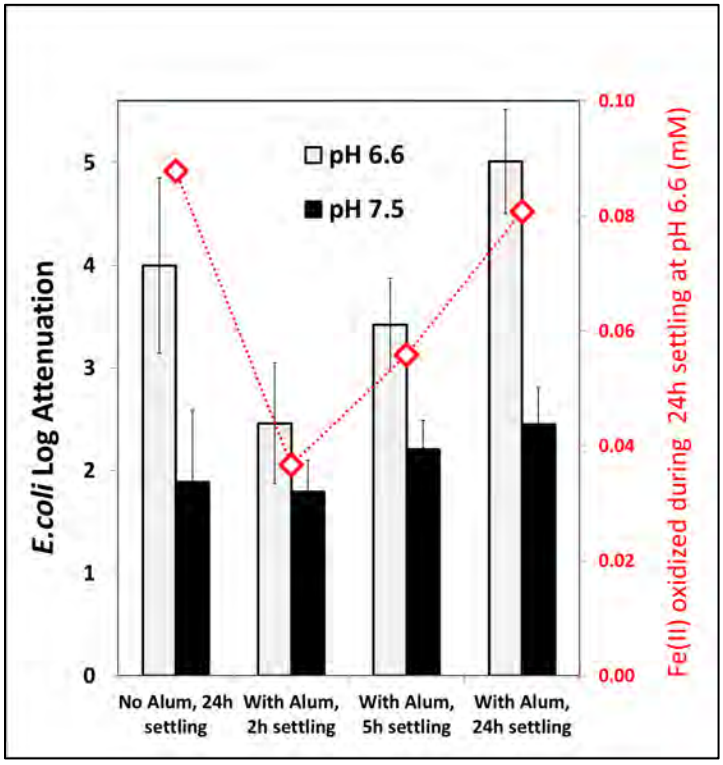

Figure 4: *E. coli* attenuation by Fe-EC as a function of settling time in experiments with alum, at pH 6.6 and 7.5 (bars). Diamonds indicate the amount of Fe(II) oxidized during the 24h settling period at pH 6.6. For comparison, results for regular Fe-EC experiments (without alum) are given on the left. The Fe dosage for all experiments was 0.5 mM.

Published in Environmental Sci. and Technology (ACS), July 2015.
DOI:10.1021/acs.est.5b01696

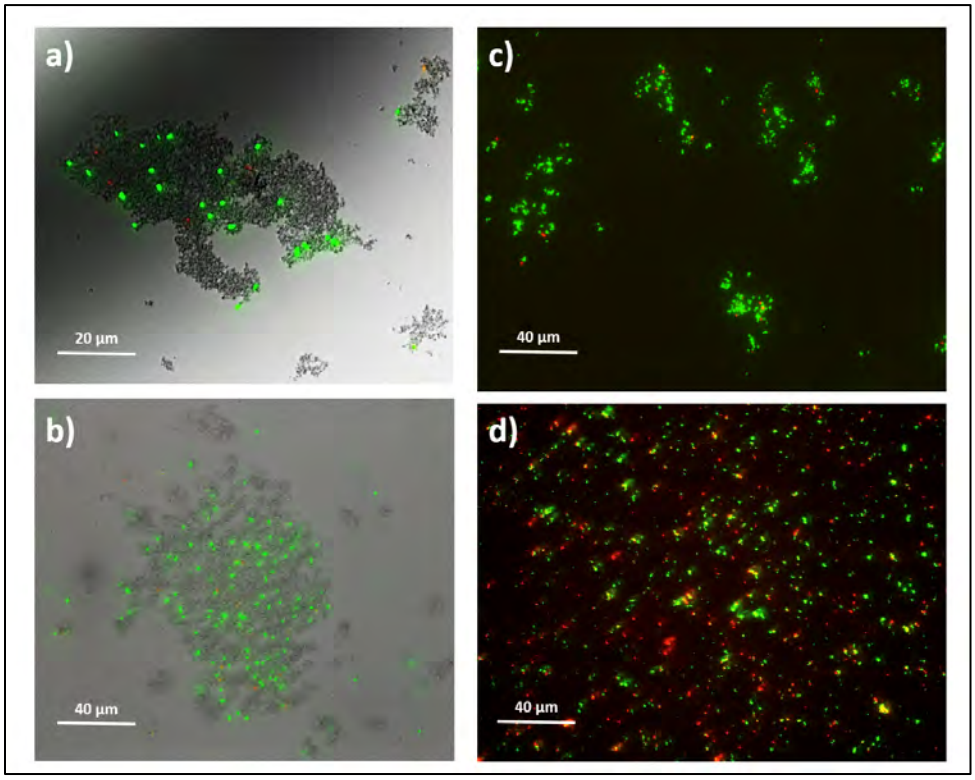

Figure 5: Fluorescent microscopy images of live-dead stained *E. coli* cells (green=live, red=dead) after dosing-mixing before settling (a, b and c). On a) and b), EC precipitate flocs are visible in grey, surrounding *E. coli* cells. a) *E. coli* counts: $10^{6.3}$ CFU/mL, pH 7.5, Fe dosage=1.5 mM. b) *E. coli* counts: $10^{6.5}$ CFU/mL, pH 6.6, Fe dosage=0.5 mM. c) *E. coli* counts: $10^{7.2}$ CFU/mL, pH 6.6, Fe dosage=0.5 mM. Figure 5d shows live-dead staining of $10^{7.6}$ CFU/mL *E. coli* left overnight at pH 6.6 with 0.18 mM $FeSO_4$ to mimic supernatant conditions.

Published in Environmental Sci. and Technology (ACS), July 2015.
DOI:10.1021/acs.est.5b01696

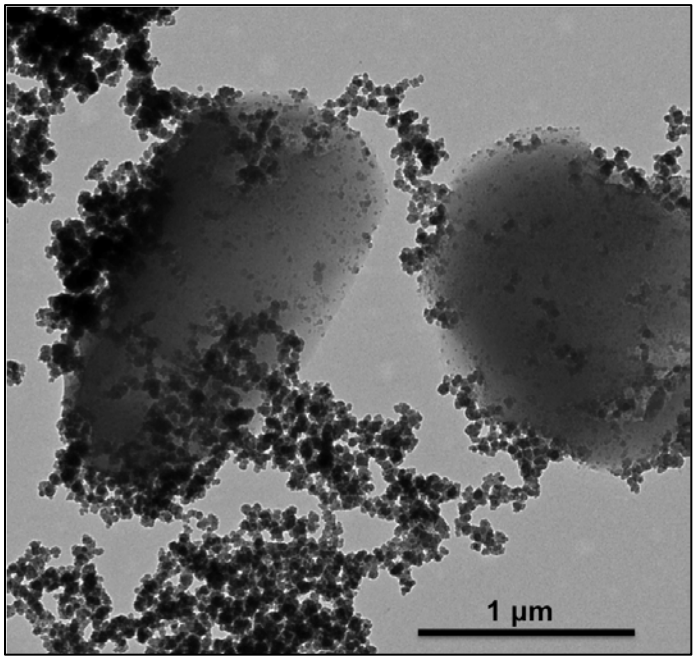

Figure 6: Transmission electron microscopy image illustrating the intimate association of EC precipitates and bacteria surfaces, with precipitates bridging two *E. coli* cells. *E. coli* counts: $10^{7.2}$ CFU/mL, Fe dosage=0.5 mM, pH 6.6.